

Article

Analyzing the Relationship between Compressive Strength and Modulus of Elasticity in Concrete with Ladle Furnace Slag

Víctor Revilla-Cuesta ¹, Roberto Serrano-López ¹, Ana B. Espinosa ², Vanesa Ortega-López ¹
and Marta Skaf ^{2,*}

¹ Department of Civil Engineering, University of Burgos, 09001 Burgos, Spain; vrevilla@ubu.es (V.R.-C.); robertosl@ubu.es (R.S.-L.); vortega@ubu.es (V.O.-L.)

² Department of Construction, University of Burgos, 09001 Burgos, Spain; aespinosa@ubu.es

* Correspondence: mskaf@ubu.es; Tel.: +34-947-259399

Abstract: The addition of Ladle Furnace Slag (LFS) to concrete modifies its compressive strength and modulus of elasticity and consequently impacts their relationship. This research evaluated both properties at 28, 90, and 180 days in concrete mixes produced with 5%, 10%, and 20% of two LFS types, both stabilized and non-stabilized. The relationship between them was then analyzed through these experimental results by adopting a statistical approach. A three-way analysis of variance revealed that both properties were affected by LFS differently. Thus, the effect of each LFS content on both features varied depending on its composition and pre-treatment. Furthermore, the effect of the LFS content on the compressive strength was also influenced by the age of the concrete. These facets implied that when analyzing the relationship between both mechanical properties, the monotonic correlations were stronger than the linear ones, reaching values between 0.90 and 1.00. Therefore, the double reciprocal regression models were the most precise ones for expressing the modulus of elasticity as a function of compressive strength. The model accuracy was further enhanced when discriminating based on the LFS type and introducing concrete age as a predictive variable. With all these considerations, the average deviations between the estimated and experimental values of 1–3% and the maximum deviations of 4–7% were reached, as well as R^2 coefficients of up to 97%. These aspects are central to the further development of LFS concrete models.

Keywords: ladle furnace slag; concrete; compressive strength; modulus of elasticity; correlations; analysis of variance; regression; time-dependent models; estimations



Citation: Revilla-Cuesta, V.; Serrano-López, R.; Espinosa, A.B.; Ortega-López, V.; Skaf, M. Analyzing the Relationship between Compressive Strength and Modulus of Elasticity in Concrete with Ladle Furnace Slag. *Buildings* **2023**, *13*, 3100. <https://doi.org/10.3390/buildings13123100>

Academic Editors: Ciro Del Vecchio and Cedric Payan

Received: 6 November 2023

Revised: 20 November 2023

Accepted: 12 December 2023

Published: 13 December 2023



Copyright: © 2023 by the authors. Licensee MDPI, Basel, Switzerland. This article is an open access article distributed under the terms and conditions of the Creative Commons Attribution (CC BY) license (<https://creativecommons.org/licenses/by/4.0/>).

1. Introduction

Compressive stresses are best withstood by concrete due to its high compressive strength [1], which is in fact the basis for the design of concrete elements under failure conditions [2–4], regardless of the nature of the reinforcement used [5]. Moreover, compressive strength is the most readily measurable mechanical property of concrete in the quality control of a concrete plant [6]; this is because its determination only requires a press with the appropriate load capacity, without the need for any other specific equipment [7,8]. The modulus of elasticity is also a key property in the design of concrete elements in the context of serviceability conditions [9], whose objective is to ensure that the deformation or deflection of the concrete element is within adequate limits in order to ensure comfortable and reliable use [10]. However, the determination of the modulus of elasticity within the aforementioned quality control is more complex and costly, due to the specialized equipment required and the need for personnel with specific knowledge to carry it out [11]. Thus, it is very common to estimate the value of the modulus of elasticity as a function of the compressive strength, thus circumventing the need for this test [12]. In fact, many concrete design standards have formulas for this purpose [13,14].

The addition of alternative raw materials to concrete, mainly industrial wastes or by-products [15,16], is currently one of the main strategies to increase the sustainability of

this construction material [17,18]. These efforts to increase concrete sustainability have even led to the evaluation of the feasibility of using types of fibers other than the conventional ones [19], including natural and sustainable fibers [20]. However, their use results in a modification of the values of the mechanical properties of concrete, such as the compressive strength and modulus of elasticity. Numerous examples can be found in the literature that support this observation. For instance, some authors have noted the deterioration of both properties following the addition of recycled concrete aggregate, due to its greater flexibility and poorer adhesion to the cementitious matrix [1,11,21]. Conversely, there is a common improvement in both properties thanks to the use of electric arc furnace slag, primarily due to its high hardness and strong bond to the matrix [6,22]. In the field of binders, the effect generally depends on the type and the method of use. Hence, in general, they tend to deteriorate both properties when used as a cement replacement but can improve both when used as an addition [23,24]. Nevertheless, this behavior notably depends on the design conditions followed, irrespective of the alternative raw material under consideration [25,26].

Moreover, as the use of alternative raw materials influences the compressive strength and modulus of elasticity of concrete, it also modifies the relationship between these properties [26]. Thus, a field of research in concrete science has involved the investigation of models that accurately describe those relationships by means of statistical procedures [12,27] and, more recently, by means of programming and computational techniques [28,29]. There is therefore a need to model these relationships when non-conventional materials are used to manufacture concrete [30]. This is the case with Ladle Furnace Slag (LFS) [31].

LFS is a by-product obtained during steel refining in ladle furnaces that has the appearance of a grayish powder [32–34]. Its chemical composition is mainly based on calcium, silicon, and aluminum oxides [35–37] and is similar to that of ordinary Portland cement [38,39]. Therefore, LFS forms calcium-silicate-hydrated gels when mixed with water; thus, it develops strength [35,38] in the same way as other slag types, such as ground granulated blast furnace slag [27]. However, its composition also usually contains a significant percentage of free magnesium and calcium oxides [40], which often produce expansive reactions when mixed with water, resulting in the formation of magnesium and calcium hydroxides [41,42]. This expansivity problem can be more pronounced, as the high temperatures reached in ladle furnaces may cause the magnesium oxide in LFS to be hard-burned; consequently, it exhibits low reactivity and can undergo this expansive reaction long after being mixed with water [43,44]. Thus, LFS has traditionally been regarded as a waste material, and it is typically deposited in landfills after its stabilization through aging and water sprinkling [40,45].

In recent years, research has attempted to revalue LFS as a suitable raw material for the manufacturing of mortars [46–49] and, specifically, concrete [30,50,51]. Its addition, after proper stabilization, has proven that it has the ability to partially replace the fine aggregate, while preserving mechanical properties [31,52]. However, if LFS is added when it has only undergone partial stabilization or if it is in its virgin state, it will undergo strength-development reactions that improve the mechanical properties [53], but it will also experience expansive phenomena due to the hydration of the free magnesium and calcium oxides that will micro-crack the cementitious matrix, potentially deteriorating the mechanical behavior [54,55]. These expansive phenomena do not necessarily have to be viewed as unfavorable, as long as they are balanced with the development of strength [32,54] or occur in situations where a reduction in concrete shrinkage is desirable, as recently demonstrated, for instance, with magnesium oxide [56–58].

This study aims to advance the characterization of the behavior of concrete made with LFS; more specifically, it aims to model the relationship between its compressive strength and its modulus of elasticity. To the authors' knowledge, there is no study in the literature that deeply analyzes the relationship between these two properties in concrete produced with this by-product. To this end, concrete mixes were made with LFS contents ranging from

0% to 20% as a cement addition, in which both mechanical properties were determined at 28, 90, and 180 days. LFS from two different origins was considered. From the results of their testing and by adopting a statistical approach, the relationship between both properties was analyzed. Thus, guidelines for the precise definition of the relationship between them in LFS concrete are provided for the first time in the scientific literature. The precise definition of this relationship is essential to accurately estimate the modulus of elasticity from the compressive strength in LFS concrete, which facilitates the design of elements cast with this concrete type and, at the same time, promotes its more widespread use.

2. Materials and Methods

2.1. Raw Materials

The concrete mixes were prepared using ordinary Portland cement CEM II/A-L 42.5 R, according to EN 197-1 [59]; water; a plasticizer; a viscosity regulator; two different types of aggregates; and LFS.

Regarding the aggregates, washed siliceous aggregate 0/16 mm with a continuous particle size was used; it was supplied by a construction materials company and specifically utilized for concrete manufacture. However, the fines content (particles smaller than 0.1 mm) of this aggregate was considered insufficient to reach adequate workability when adding LFS, due to the rougher surface of LFS compared to conventional aggregates [54]. To address this, the siliceous aggregate was supplemented with limestone sand 0/2 mm, with a higher fines content. All the physical properties of the two aggregates (Table 1) were in accordance with the common values [1,13], and their fineness modulus supported the previous observations regarding the fines content.

Table 1. Aggregate physical properties as per EN 933-1 [59] and EN 1097-6 [59].

Aggregate	Density (kg/m ³)	Water Absorption (% wt.)	Fineness Modulus
Siliceous 0/16 mm	2.59/2.70 ¹	1.8/0.2 ¹	5.85
Limestone 0/2 mm	2.66	0.1	2.73

¹ Values for the 4/16 mm and 0/4 mm fractions, respectively.

Two types of LFS 0/2 mm were considered and were denoted as *S* and *NS* in this study. Their physical properties (Table 2) showed the usual values for this by-product [35,36]. On the one hand, the LFS labelled as *S* was provided by a waste management company and was partially stabilized before being supplied by exposure to environmental conditions, regular watering, and periodic turning. On the other hand, the LFS named *NS* was sourced from a ladle furnace and had only received brief water irrigation for cooling, without undergoing intensive stabilization. In view of these different supply conditions, it was expected that the *NS*-type LFS would exhibit greater chemical activity when used in concrete [40], as explained in the introduction. In addition, it was also probable that this type of LFS would have a higher potential for expansive phenomena due to its higher MgO content, as revealed from the chemical composition analyses performed by X-ray fluorescence (Figure 1).

Table 2. LFS physical properties as per EN 933-1 [59] and EN 1097-6 [59].

LFS Type	Density (kg/m ³)	Water Absorption (% wt.)	Fineness Modulus
Stabilized	2.68	0.4	2.60
Non-stabilized	2.74	1.4	1.86

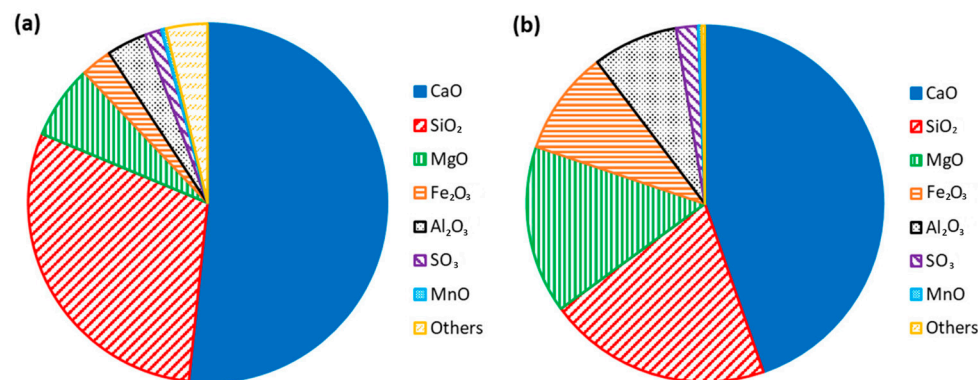


Figure 1. Chemical composition through X-ray fluorescence: (a) stabilized LFS; (b) non-stabilized LFS.

2.2. Mix Design

The concrete mixes were designed to consistently reach a slump class S2 in accordance with EN 206 [59] and, more specifically, a slump value of 8 ± 2 cm. However, the aim was also for the concrete to achieve a 28-day compressive strength of at least 35 MPa. These levels of workability and compressive strength are common in conventional vibrated concrete and thus give the mixes a wide applicability [13,14].

These design objectives were met in the reference mix by empirically establishing a cement content of 320 kg/m^3 , a water/cement ratio of 0.46, and an admixture content of 1.9% by weight of cement. In addition, the amounts of each aggregate were defined so that the content of particles smaller than 0.1 mm was around 8% of the total aggregate volume, which is a suitable proportion according to other studies [46,52].

The design of the concrete mixes with LFS was conducted by considering this by-product as a cement addition. Thus, 5%, 10%, and 20% of the volume of the limestone sand 0/2 mm was replaced by each type of LFS 0/2 mm. These LFS contents were defined on the basis of studies collected from the literature which aimed to optimize the benefits of LFS in terms of strength development while minimizing the risk of the deterioration of the concrete performance by expansive processes [25,32,53]. To maintain the workability in the desired range, the water content was slightly increased when both types of LFS were added, although this compensation had to be higher for the NS-type LFS due to its higher water-absorption levels (Table 2).

The concrete mixes were denoted as “XS” or “XNS” for the stabilized and non-stabilized LFS, respectively. X represented the percentage content of LFS. The reference mix was named OR, thus indicating that it incorporated a 0% LFS content. The mix design of the seven concrete mixes produced is detailed in Table 3.

Table 3. Mix design (kg/m^3).

Mix	Cement	Water	Plasticizer	Viscosity Regulator	Siliceous # Limestone Aggregate	LFS
0R	320	149	4.0	2.0	1750 # 320	0
5S	320	151	4.0	2.0	1750 # 304	16 ¹
10S	320	152	4.0	2.0	1750 # 288	32 ¹
20S	320	156	4.0	2.0	1750 # 256	65 ¹
5NS	320	154	4.0	2.0	1750 # 304	16 ²
10NS	320	156	4.0	2.0	1750 # 288	32 ²
20NS	320	162	4.0	2.0	1750 # 256	65 ²

¹ Amounts of stabilized LFS. ² Amounts of non-stabilized LFS.

2.3. Experimental Tests

Cylindrical specimens of 10×20 cm were prepared for all the mixtures. These specimens remained in the laboratory environment for 24 ± 1 h after casting and were subsequently stored in a wet chamber that complied with the requirements of EN 12390-2 [59]

until the different testing points. Compressive strength and modulus of elasticity were measured in three specimens at each of the following intervals: 28, 90, and 180 days, in accordance with the standards EN 12390-3 [59] and EN 12390-13 [59], respectively. A wide time range was selected to precisely evaluate the effect of LFS on the temporal evolution of both mechanical properties [32]. The results of these tests were the basis for the development of the entire analysis of the relationship between both properties in the LFS concrete mixes.

2.4. Formulas of the Regulations

Nearly every design standard for concrete elements contains formulas for estimating the modulus of elasticity based on the compressive strength. Arguably, the two most well-known and widely used formulas are those found in the European (Eurocode 2 [13]) and North American (ACI 318-19 [14]) standards [26,27], as shown in Equation (1) and Equation (2), respectively. In these expressions, ME is the modulus of elasticity of concrete in GPa; CS is the compressive strength of concrete in MPa (for the Eurocode 2 [13], this strength is always at 28 days); and t is the time in days.

$$ME = 21.5 \times \left(\exp \left\{ 0.2 \times \left[1 - \left(\frac{28}{t} \right)^{0.5} \right] \right\} \right)^{0.5} \times \left(\frac{CS_{28}}{10} \right)^{0.3} \quad (1)$$

$$ME = 4.7 \times \sqrt{CS} \quad (2)$$

The first approach used to evaluate the relationship between the compressive strength and the modulus of elasticity in LFS concrete checked whether these expressions were valid for the experimental results obtained.

2.5. Statistical Analyses

The analysis of the relationship between the compressive strength and the modulus of elasticity proceeded with the development of statistical models that linked both properties, based on the experimental results. For this purpose, four progressive steps were implemented:

1. Analysis of the significance of each factor (LFS content, LFS type, and concrete age) and their interactions with the values of the compressive strength and modulus of elasticity of concrete. To this end, a three-way analysis of variance (ANOVA) was applied with a confidence level of 95% by using all the replicates for an accurate evaluation of the dispersion of the experimental results [60].
2. Evaluation of the existence of a dependence relationship between both mechanical properties by a study of correlations. Pearson, Spearman, and Kendall correlations were considered to model all the possible interrelationships between them [61].

From these two steps, the fundamental aspects were established for the development of models that relate the compressive strength and the modulus of elasticity, and they were addressed in the following two steps. These steps were defined on the basis of the conclusions reached with the three-way ANOVA in relation to the relevance of the concrete age to both properties.

3. Development of simple regression models not dependent on the concrete age. In these models, the compressive strength was the independent variable, and the modulus of elasticity was the dependent variable.
4. Development of multiple regression models dependent on concrete age. Again, the independent variable was the compressive strength, and the dependent variable was the modulus of elasticity, but variable adjustment coefficients dependent on the age of concrete were introduced.

Finally, it should be noted that this study does not aspire to develop models that are universally valid for predicting the modulus of elasticity from the compressive strength in

concrete containing LFS. A larger volume of data would be needed for the development of this type of model; such data are not yet available in the scientific literature [31,35,40]; so, it would be necessary to continue researching the LFS concrete to this end. The objective of this study is to lay the foundations from which to start when developing these models; this is the first fundamental step in this modeling process. Thus, the key aspects that condition the relationship between the two mechanical properties are highlighted.

3. Results and Discussion

3.1. Experimental Results

The average results of the compressive strength and modulus of elasticity at 28, 90, and 180 days are listed in Table 4. The strength values generally exceeded 35 MPa, and the modulus of elasticity exceeded 30 GPa, which aligned the mixes with the characteristics of conventional concrete in terms of compressive behavior [13,14].

Table 4. Compressive strength and modulus of elasticity of the concrete mixes.

Mix	Compressive Strength			Modulus of Elasticity		
	28 Days	90 Days	180 Days	28 Days	90 Days	180 Days
OR	37.0	42.5	46.6	35.1	37.7	38.8
5S	41.6	42.7	45.9	36.9	39.0	39.7
10S	41.3	41.2	45.5	37.6	40.0	40.6
20S	39.9	41.8	44.2	39.1	43.7	44.9
5NS	47.4	48.0	50.6	39.6	42.1	41.7
10NS	44.5	45.4	50.8	38.6	40.7	41.8
20NS	34.5	39.3	44.4	32.7	34.5	34.2

With regard to compressive strength, the employment of stabilized LFS resulted in an increase in the 28-day strength (37.0 MPa for the OR mix and 41.6 MPa and 41.3 MPa for the 5S and 10S mixes, respectively). This improvement was attributed to the formation of additional calcium-silicate-hydrates during LFS hydration [53], although this hydration may also lead to the expansive phenomena (hydration of free magnesium and calcium oxides to form magnesium and calcium hydroxides) that caused minor micro-cracking of the cementitious matrix and thus counteracted the increase in strength with the higher LFS contents (39.9 MPa for the 20S mix) [36,41]. The use of non-stabilized LFS led to higher strength fluctuations due to its heightened chemical activity [40]. Thus, 5% and 10% of this LFS caused an intensified increase in the 28-day compressive strength, reaching a strength of 47.4 MPa in the 5NS mix. However, the expansive phenomena were also of greater magnitude, and they counteracted the positive effects; so, the 28-day compressive strength of the 20NS mix was only 34.5 MPa. The passage of time seems to have favored expansive phenomena in the LFS due to hydration of the hard-burned MgO [32,43], which reduced the advantages of LFS in relation to the compressive strength of concrete. Therefore, the increase in compressive strength when LFS was used was lower with higher concrete ages. The 180-day strength of all the mixes made with stabilized LFS was lower than that of the reference mix, while the gain in strength caused by 5% and 10% of non-stabilized LFS was progressively smaller (increase of 10.9 MPa for the 5NS mix at 28 days and only 4.0 MPa at 180 days).

The behavior of concrete in the elastic field was less affected by the micro-cracking because of the expansive phenomena in the LFS, as the load applied was not enough to propagate these micro-cracks throughout the whole concrete specimen [31,40]. Therefore, the trends exhibited by the modulus of elasticity were more consistent. First, increasing the amount of stabilized LFS in the concrete continuously led to an increase in elastic stiffness at all ages, thanks to the strength-development reactions [54]. For example, the 20S mix showed a modulus of elasticity of 44.9 GPa at 180 days versus 38.8 GPa for the OR mix. In addition, the use of 5% and 10% of the non-stabilized LFS also caused an increase in the modulus of elasticity of between 2 and 5 GPa with respect to the reference mix, for the

same reasons [38]. Nevertheless, the expansive phenomena when 20% of this NS-LFS was added caused a relevant micro-cracking of the cementitious matrix [32] that did result in a decrease in the modulus of elasticity ranging from 2 to 4 GPa.

3.2. Validity of the Formulas of the Regulations

First, an evaluation was made to determine whether the formulas included in the conventional standards were valid to accurately describe the relationship between the compressive strength and the modulus of elasticity in the concrete mixes made with LFS. For this purpose, Figure 2 graphically represents the experimental results of the compressive strength and modulus of elasticity for each age of study (28, 90, and 180 days), as well as the formulas of Eurocode 2 [13] and ACI 318-19 [14]. The formula of ACI 318-19 remains the same in the three figures as it does not depend on the age of the concrete (Equation (2)). Conversely, the formula of Eurocode 2 does depend on that aspect (Equation (1)), and it estimates higher values for the modulus of elasticity as the concrete age increases [26].

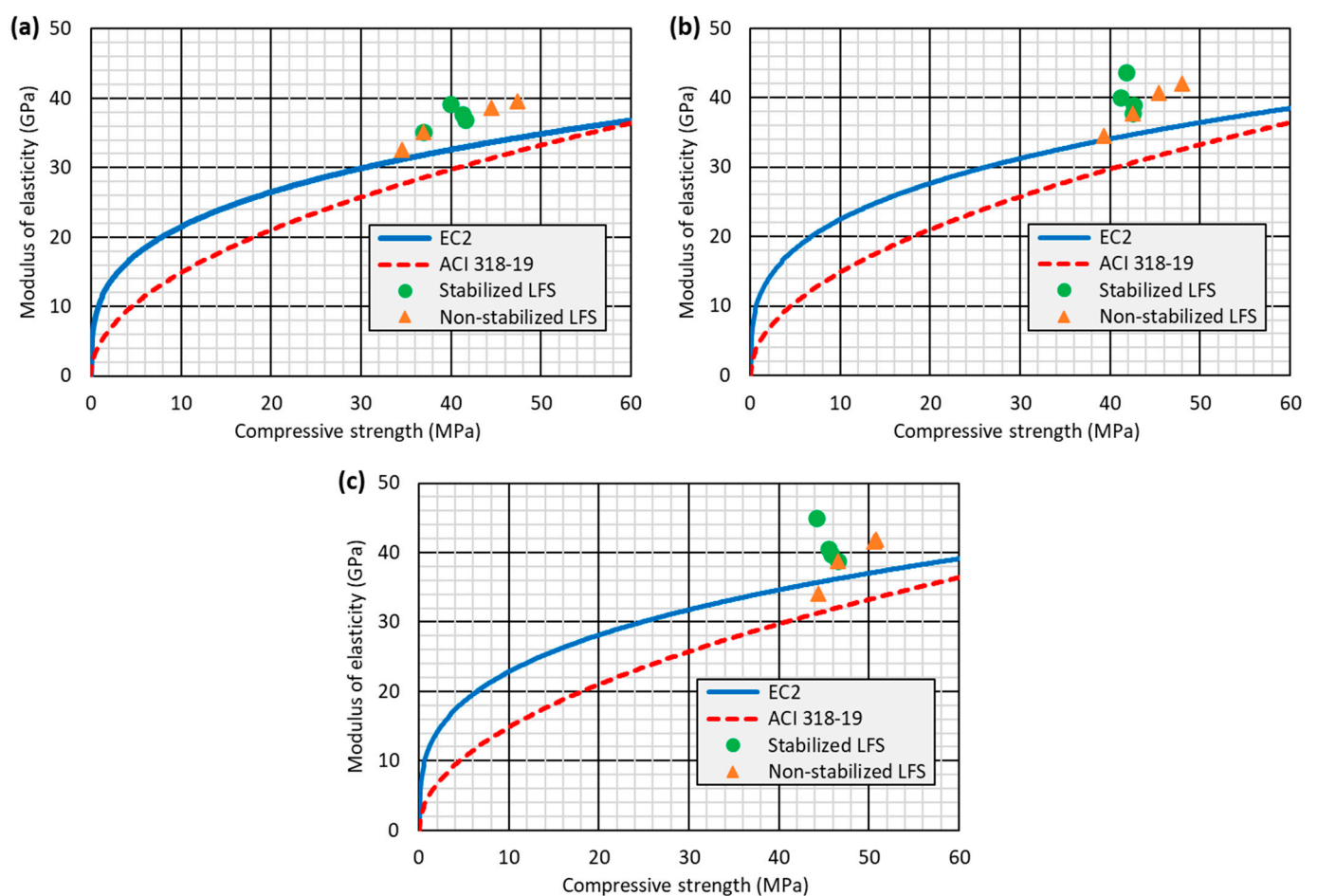


Figure 2. Comparison between the experimental results and the formulas of the standards: (a) 28 days; (b) 90 days; (c) 180 days [13,14].

As can be observed in Figure 2, the modulus of elasticity was, as usual, underestimated in all cases and thus provided a safe estimate [26]. The formula of ACI 318-19 always underestimated the modulus of elasticity of the concrete with LFS, yielding for each compressive strength a lower value of the modulus of elasticity than the experimental one. This underestimation was between 15% and 22%; this was similar for all the mixes and did not vary significantly with the concrete age. The formula of Eurocode 2 also underestimated the values of the modulus of elasticity, but to a lesser extent. In addition, the differences between the experimental and estimated values were found to be in a narrower range

when using this expression, between 8% and 12% on average, due to its ability to model the temporal increase in the modulus of elasticity [26], which was higher when adding LFS due to the strength-development reactions that it experienced [38]. However, the low values of the modulus of elasticity of the mix with 20% non-stabilized LFS, due to the aforementioned expansive phenomena [25,32], caused the formula of Eurocode 2 to overestimate the 180-day modulus of elasticity in this mix. The formula of ACI 318-19 always provided an estimation of the modulus of elasticity that was on the safe side [14], although the formula of Eurocode 2 allowed more accurate estimations.

3.3. Statistical Analyses

In view of the findings on the validity of the formulas of the regulations [13,14], further research was undertaken on the relationship between the compressive strength and the modulus of elasticity in the concrete made with LFS. The objective was to define, using a statistical approach, the basic guidelines for estimating the modulus of elasticity from the compressive strength with the highest possible accuracy.

3.3.1. Three-Way Analysis of Variance (ANOVA)

The most relevant results of the three-way ANOVA (95% confidence level) performed for the experimental results of the compressive strength and modulus of elasticity are detailed in Tables 5 and 6. These tables show the p -values that indicate the significance of each factor and their homogeneous groups (Table 5), along with the significance of the interactions (Table 6).

Table 5. Three-way ANOVA ($\alpha = 0.05$): analysis of the factors.

Factor	Compressive Strength		Modulus of Elasticity	
	p -Value	Homogeneous Groups	p -Value	Homogeneous Groups
LFS content	0.0000	None	0.0001	0% and 20%; 5% and 10%
LFS type	0.0003	None	0.0037	None
Age	0.0000	None	0.0000	90 days and 180 days

Table 6. Three-way ANOVA ($\alpha = 0.05$): analysis of the interactions.

Interaction	p -Values for Compressive Strength	p -Values for Modulus of Elasticity
LFS content–LFS type ¹	0.0000	0.0000
LFS content–Age ¹	0.0044	0.9625
LFS type–Age ¹	0.2627	0.5197
LFS content–LFS type–Age ²	0.4193	0.7040

¹ Second-order interaction. ² Third-order interaction.

All the factors were significant for both properties, although their level of significance was higher for the compressive strength. This can be explained by the fact that homogeneous groups were detected for the factors of the LFS content and concrete age with respect to the modulus of elasticity, but not for the compressive strength [26]. Thus, the addition of 0% and 20% LFS led significantly to the same values for the modulus of elasticity as the LFS contents of 5% and 10% did. Likewise, the modulus of elasticity was statistically equal at 90 and 180 days.

The interactions in an ANOVA show whether the effect of one factor is modified by varying the value of another factor [60]. In a three-way ANOVA, the third-order interaction analyzes the three factors together, while the second-order interactions analyze pairs of factors [57]. The third-order interaction was not significant for any property; so, both the compressive strength and the modulus of elasticity presented statistically equal values for various combinations of the factors. Regarding the second-order interactions, the effect of the LFS content was different for each type of LFS on both mechanical properties.

Nevertheless, the effect of the LFS content only varied with the age on the compressive strength, but not on the modulus of elasticity. This shows that the age of concrete is a fundamental aspect when establishing the relationship between the compressive strength and the modulus of elasticity in LFS concrete since it does not affect both properties in the same way. The modeling of this relationship must certainly address this issue.

3.3.2. Analysis of Correlations

A correlation analysis was conducted as a first approximation [62] of the relationship between the compressive strength and the modulus of elasticity in LFS concrete. Three types of correlations were considered, the values of which are listed in Table 7. The first was Pearson's correlation, which shows whether there is a linear relationship between two variables [63]. The second was Spearman's correlation, which indicates whether the variables show a monotonic relationship [61]. The final correlation was Kendall's correlation, which reports whether the ordering of the values of both variables is the same [64]. In all cases, an absolute value closer to 1 means that the dependence between the two variables is more intense. In addition, a positive sign indicates that the relationship between both variables is increasing, while it is decreasing when a negative sign is obtained.

Table 7. Correlations.

LFS Type	Age Condition	Pearson	Spearman	Kendall
Both together	All ages	0.65	0.61	0.47
	28 days	0.88	0.83	0.70
	90 days	0.57	0.42	0.41
	180 days	0.27	0.11	0.11
Stabilized LFS	All ages	0.44	0.38	0.27
	28 days	0.59	0.20	0.00
	90 days	−0.49	−0.60	−0.33
	180 days	−0.98	−1.00	−1.00
Non-stabilized LFS	All ages	0.88	0.91	0.76
	28 days	0.99	1.00	1.00
	90 days	0.99	1.00	1.00
	180 days	0.97	1.00	1.00

The following aspects can be noted through the values of the correlations (Table 7):

- The joint consideration of both LFS types without age differentiation led to positive correlations, indicating an increasing relationship, but with very low absolute values. If the LFS content is considered as the factor that fundamentally conditions both properties, then its effect depends on the LFS type, as explained in the three-way ANOVA (Table 5). This performance caused the relationship between both mechanical properties to follow different patterns for each LFS type [60].
- Higher correlations were obtained when separating by LFS type. However, these values were much higher when using the non-stabilized LFS. The low correlations for the stabilized LFS were because its effect on the compressive strength was lower than on the modulus of elasticity (Table 4); this behavior is also found in the literature [52]. In addition, this effect varied with concrete age, as found in the three-way ANOVA (Table 6).
- Separation by age led to stronger correlations than when it was not considered. The highest level of accuracy was achieved when separation by LFS type was simultaneously considered, as it encompassed all the significant interactions according to the ANOVA (Table 6) [57]. The correlations were almost equal to 1 at all ages for the non-stabilized LFS, whereas a greater influence of age on this relationship was found for the stabilized LFS; thus, higher values were reached at older ages. In general, the Spearman correlations provided the highest values.

In line with all the aspects described, it was first decided to proceed with the development of models that did not depend on age but differed according to the LFS type. Subsequently, the development of time-dependent models was approached. The objective was to evaluate and compare the level of accuracy and complexity of both options for modeling the relationship between the compressive strength and the modulus of elasticity in concrete with LFS.

3.3.3. Non-Time-Dependent Models

The subsequent step in the analysis was to develop models from the experimental results (Table 4) of the LFS mixes, where the modulus of elasticity (ME , in GPa) could be exclusively calculated through the compressive strength (CS , in MPa) approach described in Equation (3).

$$ME = f(CS) \quad (3)$$

Equation (3) was implemented by proposing 27 standard models that were dependent on the first power of the compressive strength. Only the first power of the compressive strength was considered in order to keep the simplicity of the application of the model [27,61]. Models were developed in which the relationship between the two variables was both directly and inversely proportional, encompassing all potential scenarios [12,62]. In addition, two different situations were addressed in this analysis. On one hand, the models were fitted by simultaneously inputting the values for all the mixes. On the other hand, the values corresponding to each LFS type were separately introduced. This approach simulated the fact that the effect of each LFS content was different for each LFS type, as shown by the three-way ANOVA (Table 5) and confirmed by the enhanced correlation values when each type of LFS was individually considered (Table 7).

All these models were adjusted by simple regression. The goodness of fit in all cases was evaluated using the R^2 coefficient since it is the most widely known indicator [60]. Thus, the linear model, for example, presented very low R^2 coefficients, ranking between the tenth and twelfth model in terms of accuracy. The model with the best average fit and R^2 coefficient was the one shown in Equation (4) (A and B , adjustment coefficients), which proposed a double reciprocal relationship between both variables. Its adjustment coefficients and the goodness-of-fit indicators for each situation are shown in Table 8. The accuracies of the models are detailed in Figure 3 through the representation of both the average and maximum deviations.

$$ME = \frac{1}{A + \frac{B}{CS}} = \frac{CS}{A \times CS + B} \quad (4)$$

Table 8. Adjustment coefficients and goodness-of-fit indicators of non-time-dependent models.

LFS Type	Coefficient A	Coefficient B	R^2 (%)	Mean Absolute Error	p -Value Durbin–Watson
Both together	0.011	0.629	48.59	0.00100	0.0832
Stabilized LFS	0.012	0.558	25.91	0.00116	0.1748
Non-stabilized LFS	0.010	0.714	76.28	0.00073	0.0693

The models developed through this analysis did not yield particularly high R^2 coefficients (Table 8). In addition, the separation based on the type of LFS had a disparate effect on this coefficient. Thus, the model in which both types of LFS were considered had an R^2 coefficient of 48.6%. When each LFS type was considered separately, this value was only improved for the non-stabilized LFS (76.3%). The model for the stabilized LFS presented a very low R^2 coefficient of 25.9%. Nevertheless, the mean absolute error was consistently low and similar in all cases, and the p -value of the Durbin–Watson statistic remained under 0.05 (95% confidence level), which showed no correlation between the residuals and thus guaranteed the significance of the model [61].

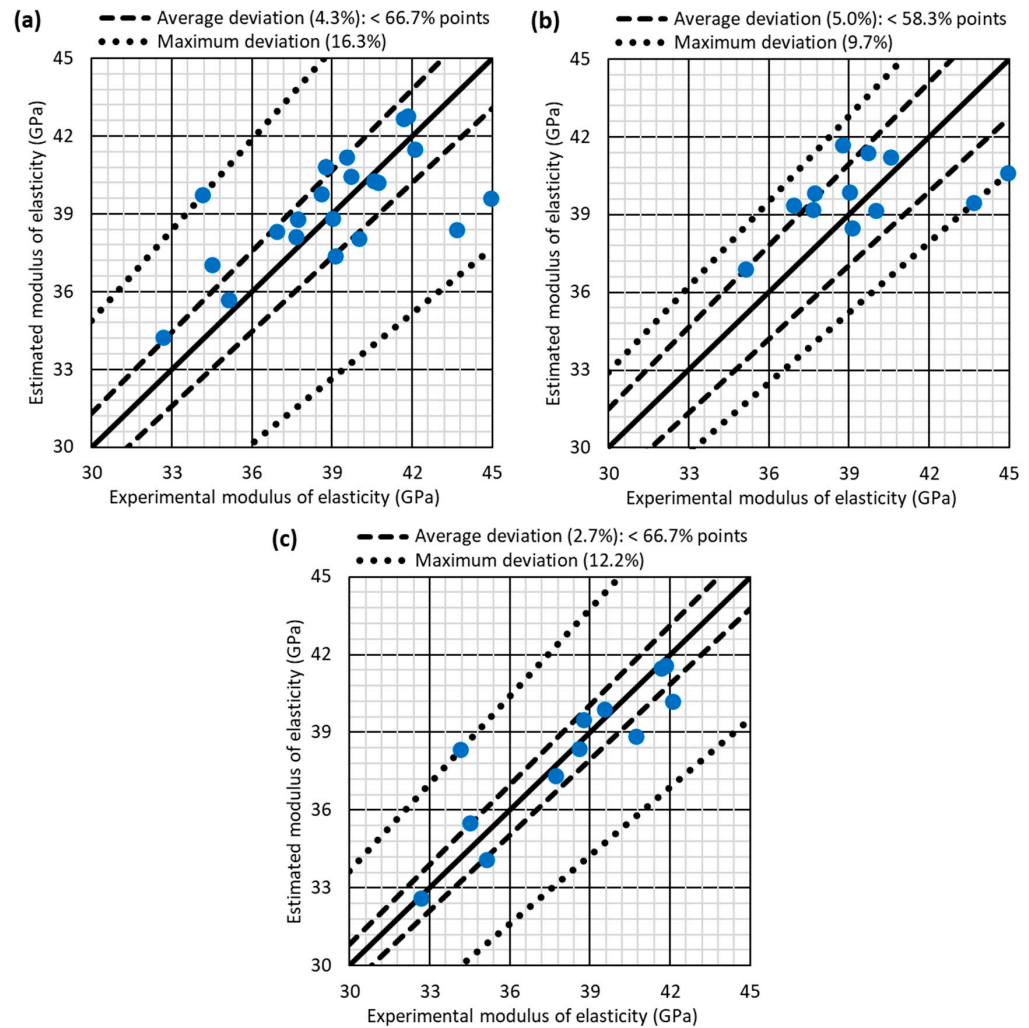


Figure 3. Comparison between the experimental elastic moduli and the values estimated through the non-time-dependent models: (a) both LFS types together; (b) stabilized LFS; (c) non-stabilized LFS.

Despite the behavior shown by the R^2 coefficients, the accuracy of the statistical modeling always improved when differentiating by LFS type (Figure 3). When both LFS types were simultaneously considered, the average and maximum deviations were 4.3% and 16.3%, respectively. However, when considering the separation between the LFS types, the average deviation remained approximately constant (5.0% for the stabilized LFS and 2.7% for the non-stabilized LFS), but the maximum deviation was significantly reduced, obtaining values of 9.7% and 12.2% for the stabilized and non-stabilized LFS, respectively. Moreover, the percentage of experimental points whose deviation from the estimated value of the modulus of elasticity was less than the average deviations was almost the same in all cases.

The trends shown by all these evaluated aspects confirmed that the relationship between the compressive strength and the modulus of elasticity in concrete with LFS can be successfully modeled using a statistical approach. However, the differentiation between the types of LFS used seems to be key to improving the estimation accuracy since their effects on the mechanical properties of concrete were different due to their varied chemical compositions [32,41] and pre-treatments [55]. In addition, it was also noted that this relationship appears to be clearer when LFS with higher chemical activity is used as it affects the concrete behavior more noticeably [53]. Therefore, in view of the low R^2 coefficient obtained in the model for stabilized LFS, it was decided to evaluate the relevance of concrete age when modeling this relationship since the three-way ANOVA showed that the effect of each LFS amount on the compressive strength changed with age (Table 6).

3.3.4. Time-Dependent Models

The best-fitting model, which is shown in Equation (4), was the basis for defining the time-dependent models. First, the trends exhibited by the adjustment coefficients A and B were analyzed through this model, which was adjusted by simple regression from the experimental results (Table 4) but was differentiated according to the concrete age (28, 90 and 180 days). Furthermore, as in the analysis of the non-time-dependent models and following the indications of the three-way ANOVA (Table 6), this study was performed both for the experimental results of both LFS types together and for the experimental results of each LFS type separately. The values of the coefficients that depended on the concrete age in each case are depicted in Figure 4.

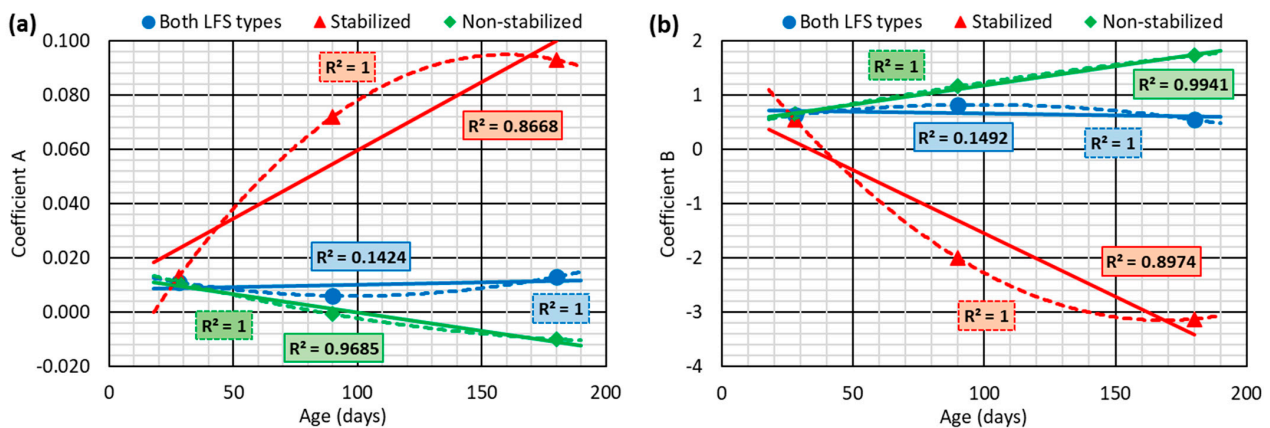


Figure 4. Adjustment coefficients of the model in Equation (4) when separating by age: (a) coefficient A ; (b) coefficient B .

As three different concrete ages were analyzed, three values were obtained for each coefficient, as shown in Figure 4. Therefore, their trends with respect to the concrete age could be optimally adjusted to a second-degree polynomial, i.e., by using a linear model with second-order time powers. The key aspect regarding the performance of the values of these coefficients was found in relation to the shape of the second-order polynomial adjustments. On one hand, the shapes of the polynomial adjustments were clearly concave/convex when both LFS types were simultaneously considered; thus, they were growing/decreasing for the early ages and subsequently presenting variations of the opposite sign. This meant that, in this case, no other type of model was found to adequately fit the trend shown by these coefficients. On the other hand, the situation was different when each LFS type was individually considered; in these cases, the variation in the coefficients with the concrete age continuously increased or decreased, especially for the non-stabilized LFS. Because of this, the evolution of the adjustment coefficients with age could be successfully fitted by a linear model dependent on first-order time powers, which is widely accepted to be the easiest regression model to work with [12,27]. All these aspects can be seen in Figure 4.

Based on the aspects indicated above, the model shown in Equation (5) was proposed as a time-dependent model to estimate the modulus of elasticity (ME , in GPa) from the compressive strength (CS , in MPa) in the concrete with LFS. This model respected the formulation of the non-time-dependent model with the best fit (Equation (4)), but an adjustment coefficient C in the numerator and two time-dependent adjustment coefficients $A(t)$ and $B(t)$ were established. These time-dependent coefficients were represented by second-order polynomial functions, as shown in Equations (6) and (7), according to the aspects previously discussed.

$$ME = \frac{C}{A(t) + \frac{B(t)}{CS}} \quad (5)$$

$$A(t) = A_0 + A_1 \times t + A_2 \times t^2 \quad (6)$$

$$B(t) = B_0 + B_1 \times t + B_2 \times t^2 \quad (7)$$

This model was fitted by multiple regression following the conclusions derived from the analysis of the trends of the adjustment coefficients with the concrete age. Thus, when the experimental results of both LFS types were simultaneously considered, the coefficients $A(t)$ and $B(t)$ were fitted as second-order polynomial functions. However, when the adjustment was performed for each LFS type separately, both second-order and first-order polynomial functions were considered for these coefficients, with the coefficients A_2 and B_2 being set equal to 0 in the second case. The purpose was to evaluate whether it was possible to simplify the prediction model without a significant loss of estimation precision. The adjustment coefficients shown in Table 9 were obtained by means of these procedures, while the goodness of fit of the resulting models is displayed in Table 10. The average and maximum deviations are depicted in Figure 5.

Table 9. Adjustment coefficients of time-dependent models.

LFS Type	Coefficient A			Coefficient B			Coefficient C
	A_0	A_1	A_2	B_0	B_1	B_2	
Both together	52.72	−0.5555	0.0030	1411	19.90	−0.1097	3180
Stabilized LFS (first-order time powers)	29.94	0.5770	0.0000	1040	−27.56	0.0000	1940
Stabilized LFS (second-order time powers)	0.1357	−0.0088	0.0001	−12.77	0.3649	−0.0010	−6.47
Non-stabilized LFS (first-order time powers)	8.14	−0.0555	0.0000	482.0	2.95	0.0000	760.2
Non-stabilized LFS (second-order time powers)	4148	−59.14	0.1405	83562	2202	−3.44	223,206

Table 10. Goodness-of-fit indicators of time-dependent models.

LFS Type	R^2 (%)	Mean Absolute Value	Durbin–Watson Statistic ¹
Both together	47.93	1.4008	1.7096
Stabilized LFS (first-order time powers)	63.00	1.2840	2.1046
Stabilized LFS (second-order time powers)	74.18	0.9548	2.5501
Non-stabilized LFS (first-order time powers)	87.20	0.9111	1.9311
Non-stabilized LFS (second-order time powers)	96.58	0.4582	2.1944

¹ Lower value of the Durbin–Watson statistic for no correlation of the residuals equal to 1.5776.

The introduction of concrete age as a variable for estimation slightly improved the prediction accuracy (Figure 5), reducing both the average and the maximum deviations by around 2% in absolute value compared to the non-time-dependent models (Figure 4). In addition, two other aspects could be noted:

- First, as in the non-time-dependent models, the separation by LFS type reduced both types of deviations. For instance, the maximum deviation was 14.2% when both LFS types were simultaneously considered, but only 3–7% when each LFS type was separately addressed. The effect of each LFS type on the mechanical properties of concrete largely depends on its chemical composition [32] and its possible pre-treatment or stabilization [45]. These factors (chemical composition and pre-treatment of the LFS) also affect the relationship between their mechanical properties, as is the case with the relationship between the compressive strength and the modulus of elasticity.
- In addition, the consideration of the functions dependent on first-order time powers for the adjustment coefficients led to a lower estimation precision, but this could be considered almost negligible. For the stabilized LFS, the deviations remained practically unchanged, while for the non-stabilized LFS the average and maximum deviations slightly increased, by 1% and 3% in absolute value, respectively. The use of first-order time powers did not affect the proportion of estimated values that showed a deviation from their corresponding experimental values below the average deviation. Therefore, the use of first-order powers of time in this case allows the simplification of the model [27] without a great loss of precision.

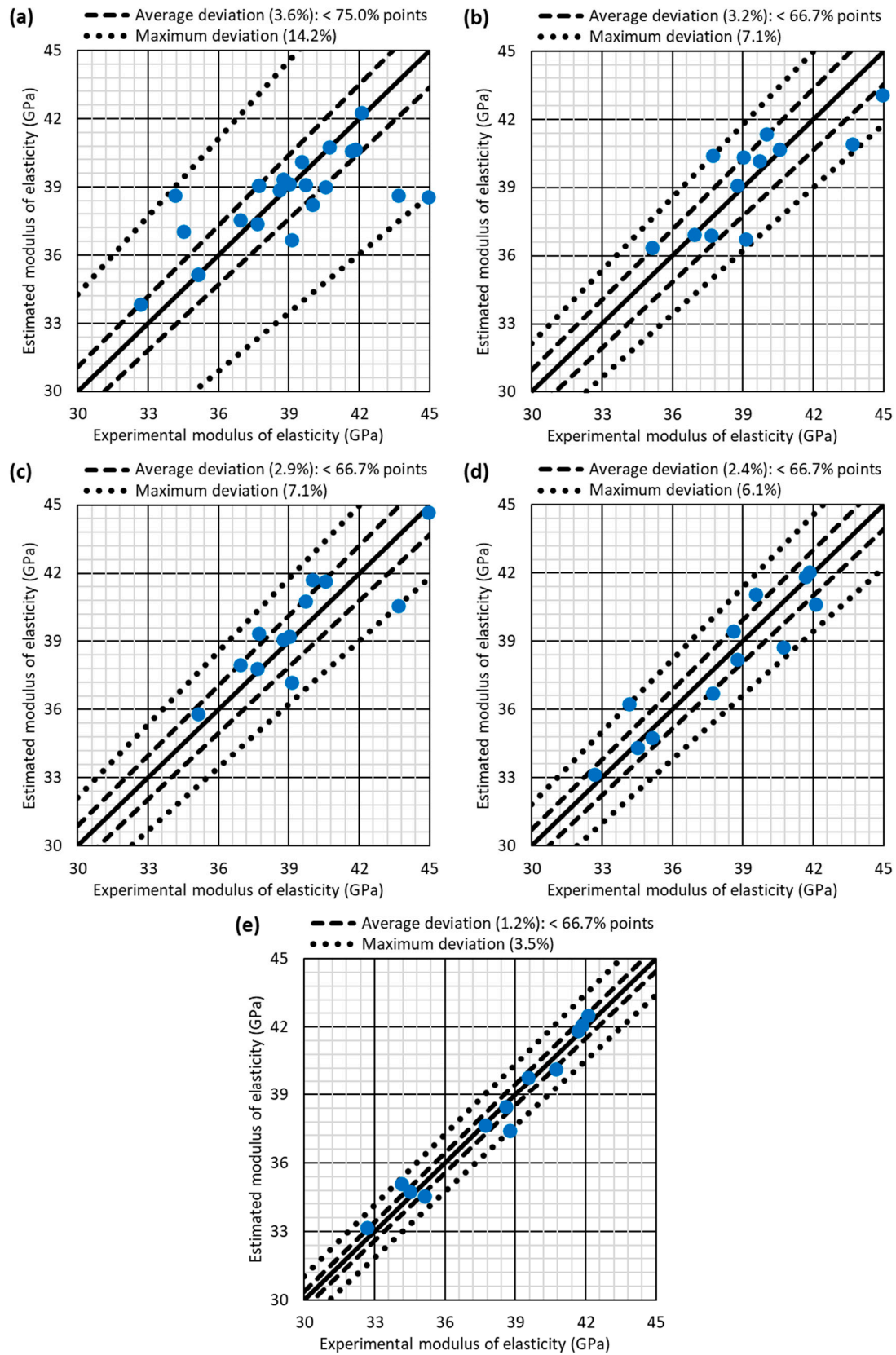


Figure 5. Comparison between the experimental elastic moduli and the values estimated through the time-dependent models: (a) both LFS types together; (b) stabilized LFS with first-order time powers; (c) stabilized LFS with second-order time powers; (d) non-stabilized LFS with first-order time powers; (e) non-stabilized LFS with second-order time powers.

All the aspects mentioned above were reflected in the obtained R^2 coefficients (Table 10); this is a very good indicator, together with the deviations, of the estimation precision and the quality of the adjustment [63]. The lowest R^2 coefficient was obtained when both types of LFS were considered simultaneously (47.93%). The separation by LFS type led to R^2 coefficients with a minimum value of 63%, although they were consistently around 10% lower in absolute value when using first-order powers of time. This performance was not reflected in the deviations. In all cases, the mean absolute error was adequate, with no large variations between the different cases studied. Finally, the Durbin–Watson statistic always showed the absence of correlation between the residuals.

4. Conclusions

Throughout this paper, the key aspects to be considered regarding the relationship between the compressive strength and the modulus of elasticity in concrete made with Ladle Furnace Slag (LFS) were analyzed using a statistical approach for the first time in the scientific literature. This relationship was evaluated in concrete mixes with workability and strength levels suitable for any use. It was evaluated using contents of 0%, 5%, 10%, and 20% of the two LFS types, both stabilized and non-stabilized, as a cement addition and by considering three different concrete ages (28, 90 and 180 days). The following main conclusions can be drawn from this analysis:

- With regard to the formulas presented in the standards, the Eurocode 2 formula [13] demonstrated superior accuracy in estimating the modulus of elasticity of LFS concrete from the compressive strength. However, this formula occasionally overestimated this mechanical property; so, the formula of ACI 318-19 [14] provided a more conservative estimation, enhancing the safety of the prediction.
- In general, the Pearson and Spearman correlations between the compressive strength and the modulus of elasticity yielded similar values, although the monotonic correlations were slightly higher. Nevertheless, in regression terms, the goodness of fit of the linear model was very low, and the best estimative approach was a double reciprocal model that was dependent on the first power of compressive strength.
- The chemical composition of the LFS and the pre-treatment it may have undergone prior to its addition to concrete resulted in the varying effects of each LFS type on the mechanical behavior of concrete. This was revealed by the significance of the interaction between the content and type of LFS according to the analysis of variance (ANOVA). Thus, a more accurate estimation of the modulus of elasticity from the compressive strength was achieved when models were developed for each LFS type separately. This was also corroborated by the increased value of the correlations observed.
- Concrete age modified the effect of LFS on compressive strength, as shown by the fact that the interaction between the LFS content and the concrete age was significant according to the ANOVA. Thus, the introduction of the age of concrete as an independent variable when estimating the modulus of elasticity separately from the compressive strength allowed a considerable improvement in the estimation accuracy.
- The functions dependent on the concrete age in the estimation models had a linear nature that was dependent on the second power of time. However, when each LFS type was considered separately, these functions could be simplified by considering only first-order powers of time, which did not noticeably affect the precision of the estimations.

Developing separate models for each LFS type, without including the concrete age as an estimative variable, made it possible to reach the mean and maximum deviations of the estimated value of the modulus of elasticity with respect to the experimental one of 3–5% and 10–12%, respectively. When the age of concrete was additionally introduced as an estimative variable, these deviations were even lower, with values of 1–3% and 4–7%, respectively. With both methods, adequate estimation accuracy was reached.

Future research lines should address the analysis of the compressive strength and modulus of elasticity of concrete by incorporating other LFS types of different origins and subjecting them to diverse pre-treatments. This would contribute to the advancement of

the research on this by-product and provide more data to develop more general models for predicting the modulus of elasticity of LFS concrete from its compressive strength by applying the findings presented in this study.

Author Contributions: Conceptualization, V.R.-C. and M.S.; methodology, R.S.-L., A.B.E. and M.S.; software, V.R.-C., R.S.-L. and A.B.E.; validation, R.S.-L. and A.B.E.; formal analysis, V.R.-C., R.S.-L. and A.B.E.; investigation, V.R.-C., R.S.-L. and A.B.E.; resources, V.O.-L. and M.S.; data curation, V.R.-C., R.S.-L. and A.B.E.; writing—original draft preparation, V.R.-C.; writing—review and editing, V.O.-L. and M.S.; visualization, V.R.-C. and V.O.-L.; supervision, V.O.-L. and M.S.; project administration, V.O.-L. and M.S.; funding acquisition, V.O.-L. and M.S. All authors have read and agreed to the published version of the manuscript.

Funding: This research was funded by the Spanish Ministry of Universities, MICIN, AEI, EU, ERDF, and NextGenerationEU/PRTR, grant numbers PID2020-113837RB-I00, 10.13039/501100011033, and TED2021-129715B-I00; the Junta de Castilla y León (Regional Government) and ERDF, grant number UIC-231, and BU033P23; and the University of Burgos, grant numbers SUCONS, Y135.GI.

Data Availability Statement: Data are contained within the article.

Conflicts of Interest: The authors declare no conflict of interest.

References

- Silva, R.V.; De Brito, J.; Dhir, R.K. The influence of the use of recycled aggregates on the compressive strength of concrete: A review. *Eur. J. Environ. Civ. Eng.* **2015**, *19*, 825–849. [[CrossRef](#)]
- Al-Atta, B.; Kalfat, R.; Al-Mahaidi, R. Hybrid and patch anchors for prevention of IC debonding in RC planks flexurally strengthened using FRP. *Structures* **2022**, *43*, 1042–1056. [[CrossRef](#)]
- Zheng, J.; Pan, Z.; Zhen, H.; Deng, X.; Zheng, C.; Qiu, Z.; Xie, L.; Xiong, Z.; Li, L.; Liu, F. Experimental Investigation on the Seismic Behavior of Precast Concrete Beam-Column Joints with Five-Spiral Stirrups. *Buildings* **2023**, *13*, 2357. [[CrossRef](#)]
- Zhou, C.; Wang, J.; Shao, X.; Li, L.; Sun, J.; Wang, X. The feasibility of using ultra-high performance concrete (UHPC) to strengthen RC beams in torsion. *J. Mater. Res. Technol.* **2023**, *24*, 9961–9983. [[CrossRef](#)]
- Sun, L.; Wang, C.; Zhang, C.; Yang, Z.; Li, C.; Qiao, P. Experimental investigation on the bond performance of sea sand coral concrete with FRP bar reinforcement for marine environments. *Adv. Struct. Eng.* **2023**, *26*, 533–546. [[CrossRef](#)]
- Revilla-Cuesta, V.; Fiol, F.; Perumal, P.; Ortega-López, V.; Manso, J.M. Using recycled aggregate concrete at a precast-concrete plant: A multi-criteria company-oriented feasibility study. *J. Clean. Prod.* **2022**, *373*, 133873. [[CrossRef](#)]
- Kouddane, B.; Sbartai, Z.M.; Elachachi, S.M.; Lamdouar, N. New multi-objective optimization to evaluate the compressive strength and variability of concrete by combining non-destructive techniques. *J. Build. Eng.* **2023**, *77*, 107526. [[CrossRef](#)]
- Xu, D.; Tang, J.; Hu, X.; Yu, C.; Han, F.; Sun, S.; Deng, W.; Liu, J. The influence of curing regimes on hydration, microstructure and compressive strength of ultra-high performance concrete: A review. *J. Build. Eng.* **2023**, *76*, 107401. [[CrossRef](#)]
- Barros, H.; Ferreira, C.; Figueiras, J. Serviceability design of reinforced concrete members—Closed form solution. *Eng. Struct.* **2013**, *49*, 600–605. [[CrossRef](#)]
- Honfi, D.; Mårtensson, A.; Thelandersson, S. Reliability of beams according to Eurocodes in serviceability limit state. *Eng. Struct.* **2012**, *35*, 48–54. [[CrossRef](#)]
- Vintimilla, C.; Etxeberria, M. Limiting the maximum fine and coarse recycled aggregates-type a used in structural concrete. *Constr. Build. Mater.* **2023**, *380*, 131273. [[CrossRef](#)]
- Silva, R.V.; De Brito, J.; Dhir, R.K. Establishing a relationship between modulus of elasticity and compressive strength of recycled aggregate concrete. *J. Clean. Prod.* **2016**, *112*, 2171–2186. [[CrossRef](#)]
- EN 1992-1; EC-2 Eurocode 2: Design of Concrete Structures. Part 1-1: General Rules and Rules for Buildings. CEN (European Committee for Standardization): Brussels, Belgium, 2010.
- ACI-318-19; Building Code Requirements for Structural Concrete. American Concrete Institute: Indianapolis, IN, USA, 2019.
- Singh, A.; Wang, Y.; Zhou, Y.; Sun, J.; Xu, X.; Li, Y.; Liu, Z.; Chen, J.; Wang, X. Utilization of antimony tailings in fiber-reinforced 3D printed concrete: A sustainable approach for construction materials. *Constr. Build. Mater.* **2023**, *408*, 133689. [[CrossRef](#)]
- Slaný, M.; Kuzielová, E.; Žemlička, M.; Matejdes, M.; Struhárová, A.; Palou, M.T. Metabentonite and metakaolin-based geopolymers/zeolites: Relation between kind of clay, calcination temperature and concentration of alkaline activator. *J. Therm. Anal. Calor.* **2023**, *148*, 10531–10547. [[CrossRef](#)]
- Pellegrino, C.; Faleschini, F.; Meyer, C. Recycled materials in concrete. In *Developments in the Formulation and Reinforcement of Concrete*; Woodhead Publishing: Sawston, UK, 2019; pp. 19–54. [[CrossRef](#)]
- Idrees, M.; Ameen, A.; Shi, J.; Saeed, F.; Gencel, O. Preparation and performance optimization of eco-friendly geopolymers prepared from coarser lignite-based waste fly ash. *Constr. Build. Mater.* **2023**, *391*, 131804. [[CrossRef](#)]
- Huang, H.; Yuan, Y.; Zhang, W.; Zhu, L. Property Assessment of High-Performance Concrete Containing Three Types of Fibers. *Int. J. Concr. Struct. Mater.* **2021**, *15*, 39. [[CrossRef](#)]

20. Chen, L.; Chen, Z.; Xie, Z.; Wei, L.; Hua, J.; Huang, L.; Yap, P.S. Recent developments on natural fiber concrete: A review of properties, sustainability, applications, barriers, and opportunities. *Dev. Built Environ.* **2023**, *16*, 100255. [[CrossRef](#)]
21. Chen, W.; Xu, J.; Li, Z.; Huang, X.; Wu, Y. Load-carrying capacity of circular recycled aggregate concrete-filled steel tubular stub columns under axial compression: Reliability analysis and design factor calibration. *J. Build. Eng.* **2023**, *66*, 105935. [[CrossRef](#)]
22. Faleschini, F.; Trento, D.; Ortega-López, V.; Zanini, M.A. Shear transfer in fly ash concrete with electric arc furnace aggregates. *Mag. Concr. Res.* **2023**, *75*, 906–918. [[CrossRef](#)]
23. Tayebani, B.; Said, A.; Memari, A. Less carbon producing sustainable concrete from environmental and performance perspectives: A review. *Constr. Build. Mater.* **2023**, *404*, 133234. [[CrossRef](#)]
24. Sun, X.; Zhao, Y.; Qiu, J.; Xing, J. Review: Alkali-activated blast furnace slag for eco-friendly binders. *J. Mater. Sci.* **2022**, *57*, 1599–1622. [[CrossRef](#)]
25. Ortega-López, V.; Revilla-Cuesta, V.; Santamaría, A.; Orbe, A.; Skaf, M. Microstructure and Dimensional Stability of Slag-Based High-Workability Concrete with Steelmaking Slag Aggregate and Fibers. *J. Mater. Civ. Eng.* **2022**, *34*, 4022224. [[CrossRef](#)]
26. Revilla-Cuesta, V.; Faleschini, F.; Pellegrino, C.; Skaf, M.; Ortega-López, V. Simultaneous addition of slag binder, recycled concrete aggregate and sustainable powders to self-compacting concrete: A synergistic mechanical-property approach. *J. Mater. Res. Technol.* **2022**, *18*, 1886–1908. [[CrossRef](#)]
27. Chandru, P.; Karthikeyan, J. Models to predict the mechanical properties of blended SCC containing recycled steel slag and crushed granite stone as coarse aggregate. *Constr. Build. Mater.* **2021**, *302*, 124342. [[CrossRef](#)]
28. Buari, T.A.; Adeleke, J.S.; Olutoge, F.A.; Ayininuola, G.M.; Dahunsi, B.I.O. Approximation of elasticity modulus of groundnut shell ash-based self-consolidating high-performance concrete using artificial neural network. *Asian J. Civ. Eng.* **2023**, *24*, 947–958. [[CrossRef](#)]
29. Ahmadi, M.; Kioumars, M. Predicting the elastic modulus of normal and high strength concretes using hybrid ANN-PSO. *Mater. Today Proc.* **2023**, *in press*. [[CrossRef](#)]
30. Santamaría, A.; Ortega-López, V.; Skaf, M.; Faleschini, F.; Orbe, A.; San-José, J.T. Ladle furnace slags for construction and civil works: A promising reality. In *Waste and Byproducts in Cement-Based Materials*; Woodhead Publishing: Sawston, UK, 2021; pp. 659–679. [[CrossRef](#)]
31. Brand, A.S.; Fanijo, E.O. A review of the influence of steel furnace slag type on the properties of cementitious composites. *Appl. Sci.* **2020**, *10*, 8210. [[CrossRef](#)]
32. Santamaría, A.; González, J.J.; Losáñez, M.M.; Skaf, M.; Ortega-López, V. The design of self-compacting structural mortar containing steelmaking slags as aggregate. *Cem. Concr. Compos.* **2020**, *111*, 103627. [[CrossRef](#)]
33. Pasetto, M.; Baliello, A.; Giacomello, G.; Pasquini, E. The Use of Steel Slags in Asphalt Pavements: A State-of-the-Art Review. *Sustainability* **2023**, *15*, 8817. [[CrossRef](#)]
34. Roberto, A.; Monticelli, R.; Roncella, R.; Romeo, E.; Tebaldi, G. Swelling Potential and Performance Level of Hot Mix Asphalt Containing Not-Hydrated Ladle Furnace Steel Slags as Filler. *J. Test. Eval.* **2023**, *52*, 1–11. [[CrossRef](#)]
35. Martins, A.C.P.; Franco de Carvalho, J.M.; Costa, L.C.B.; Andrade, H.D.; de Melo, T.V.; Ribeiro, J.C.L.; Pedroti, L.G.; Peixoto, R.A.F. Steel slags in cement-based composites: An ultimate review on characterization, applications and performance. *Constr. Build. Mater.* **2021**, *291*, 123265. [[CrossRef](#)]
36. Yildirim, I.Z.; Prezzi, M. Chemical, mineralogical, and morphological properties of steel slag. *Adv. Civ. Eng.* **2011**, *2011*, 463638. [[CrossRef](#)]
37. Wu, L.; Li, H.; Mei, H.; Rao, L.; Wang, H.; Lv, N. Generation, utilization, and environmental impact of ladle furnace slag: A minor review. *Sci. Total Environ.* **2023**, *895*, 165070. [[CrossRef](#)] [[PubMed](#)]
38. Araos Henríquez, P.; Aponte, D.; Ibáñez-Insa, J.; Barra Bizinotto, M. Ladle furnace slag as a partial replacement of Portland cement. *Constr. Build. Mater.* **2021**, *289*, 123106. [[CrossRef](#)]
39. Araos, P.; Uribarri, A.; Barra, M.; Aponte, D. The Effect of Ladle Furnace Slag (LFS) Content Replacement as a Supplementary Cementitious Material in Portland Cement-Based Systems. In *RILEM Bookseries*; Springer: Berlin/Heidelberg, Germany, 2023; Volume 44, pp. 76–87. [[CrossRef](#)]
40. Jiang, Y.; Ling, T.C.; Shi, C.; Pan, S.Y. Characteristics of steel slags and their use in cement and concrete—A review. *Resour. Conserv. Recycl.* **2018**, *136*, 187–197. [[CrossRef](#)]
41. Ortega-López, V.; Manso, J.M.; Cuesta, I.I.; González, J.J. The long-term accelerated expansion of various ladle-furnace basic slags and their soil-stabilization applications. *Constr. Build. Mater.* **2014**, *68*, 455–464. [[CrossRef](#)]
42. Rodríguez, A.; Santamaría-Vicario, I.; Calderón, V.; Junco, C.; García-Cuadrado, J. Study of the expansion of cement mortars manufactured with Ladle Furnace Slag LFS. *Mater. Constr.* **2019**, *69*, e183. [[CrossRef](#)]
43. Chatterji, S. Mechanism of expansion of concrete due to the presence of dead-burnt CaO and MgO. *Cem. Concr. Res.* **1995**, *25*, 51–56. [[CrossRef](#)]
44. Zhao, J.; Liu, Q.; Fang, K. Optimization of f-MgO/f-CaO phase in ladle furnace slag by air rapidly cooling. *Mater. Lett.* **2020**, *280*, 128528. [[CrossRef](#)]
45. Fang, K.; Zhao, J.; Wang, D.; Wang, H.; Dong, Z. Use of ladle furnace slag as supplementary cementitious material before and after modification by rapid air cooling: A comparative study of influence on the properties of blended cement paste. *Constr. Build. Mater.* **2022**, *314*, 125434. [[CrossRef](#)]

46. Aponte, D.; Martín, O.S.; Barrio, S.V.; Bizinotto, M.B. Ladle steel slag in activated systems for construction use. *Minerals* **2020**, *10*, 687. [[CrossRef](#)]
47. Sultana, I.; Islam, G.M.S. Performance of Ladle Furnace Slag in Mortar under Standard and Accelerated Curing. *Adv. Civ. Eng.* **2022**, *2022*, 7824084. [[CrossRef](#)]
48. Singh, S.K.; Tiwari, N. Development of sustainable ternary cementitious binder with OPC integrating calcined clay and LF slag. *J. Build. Eng.* **2023**, *75*, 107025. [[CrossRef](#)]
49. de Freitas Cordova de Souza, E.; da Silva, T.F.; de Castro, M.A.; dos Santos Ferreira, G.C. Combined Use of Ladle Furnace Slag and Rice Husk Ash as a Supplementary Cementitious Material. *Mater. Res.* **2023**, *26* (Suppl. S1), e20230069. [[CrossRef](#)]
50. Deepak, M.; Ramalinga Reddy, Y.; Nagendra, R. Investigating the mechanical strength, durability and micro-structural properties of slag-based concrete. *Innov. Infrastruct. Solut.* **2023**, *8*, 272. [[CrossRef](#)]
51. Gaibor, N.; Leitão, D.; Miranda, T.; Cristelo, N.; Fernandes, L.; Pereira, E.N.B.; Cunha, V.M.C.F. Fiber-Reinforced Alkali-Activated Cements from Ceramic Waste and Ladle Furnace Slag without Thermal Curing. *J. Mater. Civ. Eng.* **2023**, *35*, 4023271. [[CrossRef](#)]
52. Sideris, K.K.; Tassos, C.; Chatzopoulos, A.; Manita, P. Mechanical characteristics and durability of self compacting concretes produced with ladle furnace slag. *Constr. Build. Mater.* **2018**, *170*, 660–667. [[CrossRef](#)]
53. Anastasiou, E.K.; Papayianni, I.; Papachristoforou, M. Behavior of self compacting concrete containing ladle furnace slag and steel fiber reinforcement. *Mater. Des.* **2014**, *59*, 454–460. [[CrossRef](#)]
54. Polanco, J.A.; Manso, J.M.; Setién, J.; González, J.J. Strength and durability of concrete made with electric steelmaking slag. *ACI Mater. J.* **2011**, *108*, 196–203.
55. da Silva, T.F.; Moura, M.A.N.; de Souza, E.F.C.; Ferreira, G.C.S.; Pereira, V.F.R. Influence of the cooling process on the physicochemical properties of ladle furnace slag, used in the replacement of Portland cement. *Rev. Mater.* **2022**, *27*, e20220089. [[CrossRef](#)]
56. Hu, Z.; Chang, J.; Chen, X.; Guan, Y.; Bi, W. Preparation of magnesium oxysulfate cement with semidry carbonation high calcium content light-burned magnesium (Ca-LBM). *Constr. Build. Mater.* **2023**, *408*, 133664. [[CrossRef](#)]
57. Revilla-Cuesta, V.; Evangelista, L.; de Brito, J.; Skaf, M.; Ortega-López, V. Mechanical performance and autogenous and drying shrinkage of MgO-based recycled aggregate high-performance concrete. *Constr. Build. Mater.* **2022**, *314*, 125726. [[CrossRef](#)]
58. Gonçalves, T.; Silva, R.V.; de Brito, J.; Fernández, J.M.; Esquinas, A.R. Mechanical and durability performance of mortars with fine recycled concrete aggregates and reactive magnesium oxide as partial cement replacement. *Cem. Concr. Compos.* **2020**, *105*, 103420. [[CrossRef](#)]
59. *EN-Euronorm Rue de stassart*, 36; European Committee for Standardization: Belgium, Brussels.
60. Cantero, B.; Sáez del Bosque, I.F.; Matías, A.; Medina, C. Statistically significant effects of mixed recycled aggregate on the physical-mechanical properties of structural concretes. *Constr. Build. Mater.* **2018**, *185*, 93–101. [[CrossRef](#)]
61. Revilla-Cuesta, V.; Shi, J.Y.; Skaf, M.; Ortega-López, V.; Manso, J.M. Non-destructive density-corrected estimation of the elastic modulus of slag-cement self-compacting concrete containing recycled aggregate. *Dev. Built Environ.* **2022**, *12*, 100097. [[CrossRef](#)]
62. Zhang, J.; Han, G.; Shen, D.; An, X.; Mendoz Meyre, S. A new model to predict the optimal mix design of self-compacting concrete considering powder properties and superplasticizer type. *J. Mater. Res. Technol.* **2022**, *19*, 3980–3993. [[CrossRef](#)]
63. Nguyen, T.D.; Cherif, R.; Mahieux, P.Y.; Lux, J.; Aït-Mokhtar, A.; Bastidas-Arteaga, E. Artificial intelligence algorithms for prediction and sensitivity analysis of mechanical properties of recycled aggregate concrete: A review. *J. Build. Eng.* **2023**, *66*, 105929. [[CrossRef](#)]
64. Vakharia, V.; Gujar, R. Prediction of compressive strength and portland cement composition using cross-validation and feature ranking techniques. *Constr. Build. Mater.* **2019**, *225*, 292–301. [[CrossRef](#)]

Disclaimer/Publisher’s Note: The statements, opinions and data contained in all publications are solely those of the individual author(s) and contributor(s) and not of MDPI and/or the editor(s). MDPI and/or the editor(s) disclaim responsibility for any injury to people or property resulting from any ideas, methods, instructions or products referred to in the content.